Modeling Ozone Mass Transfer in Reclaimed Wastewater

Pan Jiang[1], Hsiao-Ting Chen[1], Roger W. Babcock, Jr.[2], Michael K. Stenstrom[1]*

ABSTRACT: Ozone mass transfer in reclaimed water was evaluated at pilot scale to determine mass-transfer characteristics and reaction kinetics and to assess the use of oxygen as a surrogate to measure this process. Tests were conducted in a 40-L/min pilot plant over a 3-year period. Nonsteady-state mass-transfer analyses for both oxygen and ozone were performed for superficial gas flow rates ranging from 0.13m/min to 0.40m/min. The psi factor, which is the ratio of volumetric mass-transfer coefficients of ozone to oxygen, was determined. The decrease in oxygen transfer rate caused by contaminants in reclaimed water was only 10 to 15% compared to tap water. A simple mathematical model was developed to describe transfer rate and steady state ozone concentration. Ozone decay was modeled accurately as a pseudo first-order reaction between ozone and ozone-demanding materials. *Water Environ. Res.,* **81,** 57 (2009).

KEYWORDS: Aeration, ozone, mass transfer, water reclamation.

doi:10.2175/106143008X325782

Introduction

Ozone-based advanced oxidation processes are in gaining popularity as a method to remove pharmaceuticals, personal care products (PPCPs), and endocrine-disrupting chemicals from wastewaters (Nakada et al., 2007). This method effectively disinfects treated wastewater effluents before discharge or reuse and works well in special applications, such as laundry wastewaters from nuclear energy facilities (Mezzanotte et al., 2007; Vilve et al., 2007). The higher oxidation potential of ozone makes it a better disinfection agent than chlorine for many pathogens, especially for unsaturated compounds. Therefore, ozonation can be used to increase the biodegradability of biologically refractory compounds. Even small doses of ozone can change the structure of compounds, making them easier to break down (Brambilla et al., 1993; Ikehata and El-Din, 2004). Ozone enhances the efficiency of the biological activated carbon process in a physical-chemical water treatment plant (Chang and Chian, 1981; Khan et al., 1998a, 1998b).

Commercially available ozone generators are only capable of producing ozone concentrations of approximately 10%, which limits the available driving force for mass transfer. Therefore, prediction and optimization of mass transfer are important for the proper design of ozonation systems (Grasso, 1987). The highly reactive nature of ozone, however, makes it difficult to directly measure its mass-transfer coefficient. An oxygen surrogate, however, has been used to estimate stripping rates of volatile organic compounds (Hsieh et al., 1993a, 1993b). The oxygen mass-transfer coefficient, which is much easier to measure, may be a more effective way to predict ozone mass-transfer rates.

The limited mass-transfer data for ozone contactors that exists is often system-specific, applying to small scales or drinking water applications only (Smith and El-Din, 2002). There also is limited information available regarding full- or pilot-scale application of ozone in reclaimed wastewater. In this study, researchers performed experiments using a pilot-scale ozone contactor in reclaimed wastewater to determine mass-transfer characteristics and reaction kinetics and to evaluate use of oxygen as a surrogate for quantifying ozone transfer.

This study used the commonly found bubble-column contactor, the most popular mass-transfer method in both the United States and Europe (El-Din and Smith, 2003). Of the 40 drinking water ozone treatment facilities in the United States, 34 were equipped with fine-bubble columns (Robson and Rice, 1991). In addition to bubble columns, there are several other types of ozone contactors, including packed towers, deep U-tubes, submerged turbines, and pipeline injectors.

Mixing in the reactor is obtained from the sparging action of the gas alone for the bubble columns. The significant advantage of bubble columns is simplicity of design, which allows for easy operation and reduced maintenance because of the absence of moving parts (Deckwer et al., 1974; Marinas et al., 1993). In addition, bubble columns typically achieve high ozone transfer efficiencies. Ozone contactors treating drinking water with a depth of 5 to 6 m can achieve transfer efficiency of more than 90% (AWWA Research Foundation, 1991). For reclaimed water and wastewaters, contaminants, particularly surface active agents, can affect mass transfer. Bubbles released by the diffuser may decrease in diameter with increasing surfactant concentration, but coalescence typically will increase. The film coefficient will decrease, resulting in an overall negative effect on transfer (Stenstrom and Gilbert, 1981; Rosso and Stenstrom, 2006).

Overall transfer efficiency alone is not sufficient to evaluate the effectiveness of an ozone contactor. It is also necessary to know the concentration profile of ozone throughout the height of the contactor column (Laplanche et al., 1991; LeSauze et al., 1993). The performance of ozone disinfection is determined by both the ozone concentration in the water and the contact time in the bubble column. The U.S. Environmental Protection Agency has adopted this ''contact-time'' concept to define the degree of disinfection (Zhou, 1995). In this research, the ozone decay rate and mass-transfer coefficients were determined, and the ozone concentration profile along the column was modeled. The affects of higher oxygen and ozone demands of the reclaimed waters also were studied. All model simulations were compared to measured results.

[1] University of California, Los Angeles, California.

[2] University of Hawaii at Manoa, Honolulu, Hawaii, Civil and Environmental Engineering Department.

* University of California-Los Angeles, Civil & Environmental Engineering Dept., 5732 Boelter Hall, Los Angeles, CA 90095-1593; e-mail: stenstro@seas.ucla.edu.

Table 1—Primary characteristics of tap water and reclaimed wastewater (TOC = total organic carbon).

Characteristics	Tap water	Reclaimed wastewater
TOC, mg/L	0.36	12.5
UV absorbance at 254 nm, cm^{-1}	0.004	0.17
pH	6	7
Temperature, °C	16–23	13–21
Alkalinity, mg/L as $CaCO_3$	3.5	67

Methodology

Experimental Setup. Experiments were conducted in a countercurrent bubble column, constructed from Schedule 80 PVC (polyvinyl chloride). Gas was introduced at the bottom of the column through a single, fine-pore ceramic dome with a 20-cm diameter designed for commercial ozone service (Aercor, Brown Deer, Wisconsin). Liquid was introduced at the top of the column. The column was 650 cm tall with internal diameter of 29 cm and a water depth of 615 cm. These columns originally were used in a 40 L/min pilot water reclamation facility operated for 3 years at Lake Arrowhead, California (Madireddi et al., 1997). Five ozone contactor columns were operated in series. Two different water types were used for mass-transfer experiments. The first water was reverse-osmosis product water from the pilot plant, which was secondary wastewater effluent that had been denitrified, alum coagulated, settled, sand-filtered, ozonated, filtered with activated carbon, and then passed through nanofiltration and reverse osmosis membranes (Madireddi et al., 1997). This water had purity similar to or better than drinking water and was denoted as ''tap water.'' The second type of water came from the same source, but only received denitrification, alum coagulation, sedimentation, and sand-filtration pretreatment. This water was denoted ''reclaimed wastewater'' and was of sufficient quality to be used for nonpotable applications in California. The main characteristics of tap water and reclaimed wastewater are summarized in Table 1.

High-purity oxygen was used for oxygen transfer experiments as well as for ozone generation for the ozone mass-transfer experiments. When using tap water, the maximum ozone dosage was limited to 24 to 25 mg/L by adjusting the power input to the ozone generator. When using reclaimed wastewater, the maximum ozone dosage was set to 7 to 8 mg/L. The higher concentrations used with tap water facilitated experiments, but would not be practical with reclaimed wastewater because the high dosage would not be typical of expected operation.

Analytical Methods. The indigo method was used to analyze ozone concentrations in both gas and liquid phases (Bader and Hoigne, 1982). Absorbance was measured on a spectrophotometer (Spectronic 20, Milton Roy Co., Ivyland, Pennsylvania) at 600 nm with a path length of 1 cm. Ozone concentration was calculated based on the absorbance coefficient of 4.2 mm^{-1} per mg/L. The spectrophotometer also was used to measure UV absorbance at 254 nm (UV254). This method is sensitive at low ozone concentrations, with a detection limit of 0.002 mg/L and is subject to little interference. The dissolved oxygen concentrations were measured with dissolved oxygen meters and membrane probes (YSI Models 57 and 58, Yellow Springs Instruments, Columbus, Ohio), which were routinely calibrated by the Winkler method [American Public Health Association (APHA), 2005]. Gas-phase oxygen concentrations were measured by gas-phase oxygen meter with a micro-fuel cell (Teledyne Model 320B, City of Industry, California). Alkalinity was determined according to the Method 2320B (APHA, 2005).

A Dohrmann DC-80 Carbon Analyzer was used to determine total organic carbon (TOC) with a detection limit of 0.05 mg/L. The TOC analyzer was calibrated with a 10 mg/L potassium hydrogen phthalate solution. Inorganic carbon was eliminated by bubbling helium gas into the sample after acidification with phosphoric acid. The TOC values reported here are the averages of three replicate measurements. Because both waters were free of suspended solids, there was no need to filter the samples.

Ozone/oxygen gas samples were taken at the inlet tubing to the bubble diffuser with a glass syringe containing a valve. The valve on the syringe was locked after sampling the ozone/oxygen gas to ensure that the pressure in the syringe was the same as the pressure in the diffuser inlet. The gas was then injected into a glass bottle sealed with a septum and containing indigo reagent, phosphate buffer, and distilled water. Once the ozone/oxygen gas was injected, the bottle was shaken well for 20 to 30 s. Absorbance at 600 nm was then measured as in the indigo method procedure for liquid samples.

Oxygen Transfer Test Protocols. Non-steady state tests were conducted for oxygen mass transfer. At the end of each test, three water samples were taken at each dissolved oxygen probe position and analyzed by the Winkler method to verify the accuracy of the membrane DO probes (Standard Methods, 2005). The non-steady state method was used to obtain the volumetric mass-transfer coefficients for oxygen to compare with the ozone experimental results. The bubble column was first filled with either tap water or reclaimed wastewater. Three dissolved oxygen probes were placed 0.6 m from the top, at mid-depth, and 0.6 m from the bottom of the column. The probes were inverted (membrane up) and equipped with a stirrer to prevent trapping of individual bubbles on the membrane. Before aeration, readings from all three probes were recorded and samples were taken from the middle of the column for alkalinity, TOC, UV254, and pH analysis. Aeration with pure oxygen was then started. Liquid samples were obtained every 5 min and dissolved oxygen readings were taken every minute. The experiments ended when the dissolved oxygen reached 96% of the expected final value.

In a batch reactor, the oxygen mass balance is given by Equation 1:

$$\frac{dC}{dt} = K_L a(C^* - C) - r \tag{1}$$

Where,

C = liquid-phase oxygen concentration (mg/L),
t = time (min),
$K_L a$ = volumetric mass-transfer coefficient (min^{-1}),
C^* = steady-state saturated liquid phase oxygen concentration (mg/L), and
r = rate of oxygen reaction (mg/L-min).

At steady state, Equation 1 can be simplified as follows:

$$r = K_L a(C^* - C_{ss}) \tag{2}$$

Where,

C_{ss} = steady state liquid phase oxygen concentration (mg/L).

The value of C^* can be estimated from the experimental data or calculated from the gas-phase oxygen concentration using Henry's Law:

$$C^* = HC_g$$

Where,

H = Henry's law coefficient and
C_g = gas-phase oxygen concentration.

Ozone Transfer Test Protocols. The ozone test protocols were similar to the oxygen tests except that the feed gas was ozone and ozone concentrations rather than oxygen were measured. Non-steady-state tests were conducted for both ozone mass transfer and decomposition kinetics studies. Four gas flow rates of 2.8, 4.7, 6.6, and 8.5 L/min (6, 10, 14, and 18 ft^3/h) were reported at standard conditions of 20°C and 1 atm pressure. The bubble column was first filled with tap water or reclaimed wastewater. Before aerating the water, samples were obtained from the middle of the column for analysis of alkalinity, TOC, UV254, and pH. Samples also were obtained from both the top and bottom of the column for liquid-phase ozone concentration measurements. Next, the output of the ozone generator was fed continuously into the column through the ceramic dome diffuser. The ozone concentration in the gas phase was measured in each run by the indigo method. During ozonation, liquid samples were taken every 5 min from the top, middle, and bottom of the column. At the same time, dissolved oxygen was measured in the middle of the column. When steady-state oxygen and ozone concentrations in the liquid phase were observed, the gas stream was shut off, and liquid-phase samples were collected every 3 min and analyzed using the indigo method. The same Equations 1 and 2 apply to ozone mass transfer.

Because some physical properties are dependent on temperature—such as viscosity, density, surface tension, and molecular diffusivity—all volumetric mass transfer coefficient values (K_La) obtained at different temperatures were corrected to 20°C to allow for comparison. The conversion is as follows:

$$K_La_{(20^\circ C)} = K_La_{(T^\circ C)} \times 1.024^{(20-T)} \tag{3}$$

For convenience, the temperature subscript (20°C) will not be used in this paper, unless reference is made to K_La values at temperatures other than 20°C.

Ozone Concentration Profile Model. To evaluate the effectiveness of an ozone reactor, it is necessary to understand the concentrations of ozone over the entire height of the reactor. A mathematical model is used here to calculate the ozone concentration profile. There are several assumptions for the simulation:

- The reactor operates at steady state.
- The flow rate, interfacial area, temperature, and overall mass-transfer coefficient are constant during each experiment.
- Both gas and liquid phases behave as plug flow.
- The hydrostatic head or pressure varies linearly with water depth.
- There are no short-circuiting or dead zones.
- For a small unit of height in the reactor, the ozone concentrations in both gas and liquid phases are constant.
- Equilibrium holds at the gas-liquid interface and is described by Henry's Law.
- The ozone decay rate is pseudo first-order in the liquid phase and negligible in the gas phase.

The mass balance of ozone during mass transfer between the heights (h) and (h + dh) in the liquid phase and gas phase are:

$$C_h = C_{h+dh} + \frac{K_La(C_h^* - C_h)\varepsilon_L A dh}{Q_L} - \frac{kC_h\varepsilon_L A dh}{Q_L} \tag{4}$$

$$C_{gh} = \frac{C_{g(h+dh)} + K_La(C_h^* - C_h)\varepsilon_L A dh}{Q_g} \tag{5}$$

Where,

C_h, C_{h+dh} = liquid phase ozone concentration at height h, h+dh,
C_{gh}, $C_{g(h+dh)}$ = gas phase ozone concentration at height h, h+dh,
$K_La\ (C_h^* - C_h)\ \varepsilon_L A dh$ = amount of ozone transferred from the gas phase to the liquid phase,
$kC_hA\varepsilon_L dh$ = amount of ozone consumed because of reaction,
$k = k_1$ = first-order rate constant for ozone decomposition reaction (min^{-1}), for tap water,
k = w = reaction rate constant (min^{-1}), for reclaimed wastewater
ε_L = liquid hold-up, i.e. liquid volume/system volume,
Q_L = liquid flow rate (L/min),
Q_g = gas flow rate (L/min), and
H = 0 at the bottom of the column = 615 cm at the top of the column.

Taking limit as dh → 0, Equations 4 and 5 can be rewritten as:

$$\frac{dC}{dh} = -\frac{(K_La\varepsilon_L + k_1\varepsilon_L)C - K_La\varepsilon_L C^*}{u_L} \tag{6}$$

$$\frac{dC_g}{dh} = -\frac{K_La\varepsilon_L(C^* - C)}{u_g} \tag{7}$$

Where,

$u_L = Q_L/A$; $u_g = Q_g/A$ = liquid flow and gas flow superficial velocity, respectively, and
C^* = the saturation concentration of ozone in the liquid phase.

Let $M = \frac{K_La\varepsilon_L}{u_L}$ $N = \frac{K_La\varepsilon_L + k_1\varepsilon_L}{u_L}$,

Equations 6 and 7 can be integrated along the height of column reactor as:

$$\int_0^H d(e^{Nh}\cdot C) = \int_0^H e^{Nh}\cdot M\cdot C^*\cdot dh$$

$$\Rightarrow e^{NH}C_t - C_b = M\int_0^H e^{NH}C^*\Delta h \tag{8}$$

$$C_{gt} = C_{gt}^* - (C_{gb}^* - C_{gb})\exp(-\frac{K_La\varepsilon_L H}{u_g}) \tag{9}$$

Where,

h = the height of liquid in column reactor, with the range from 0 to the maximum
H = 615 cm, and Δh = 5 cm, and
C_t, C_b and C_{gt}, C_{gb} = liquid phase and gas phase ozone concentration at the top and bottom of reactor.

Ozone concentrations in both the water and the gaseous phase along the column were calculated using an iterative solution of Equations 8 and 9. The calculation started from the top of the column, where the liquid-phase ozone concentration was known. An arbitrary value was taken for an initial guess of gas-phase ozone concentration (Cgt) and both gas- and liquid-phase ozone concentration profiles were calculated with all the other known

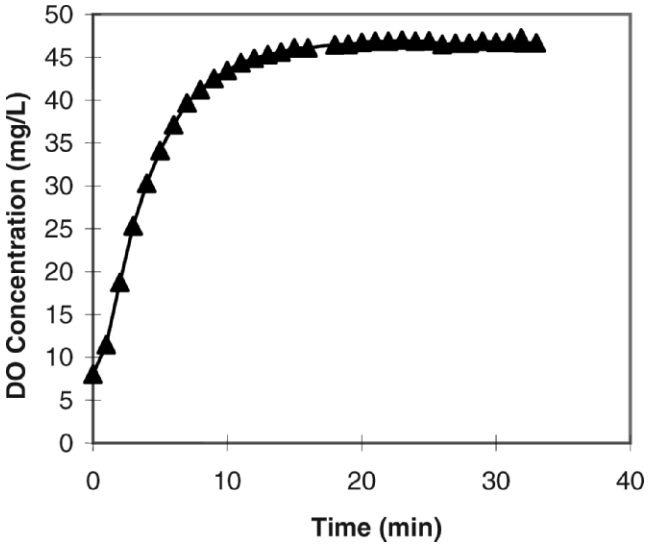

Figure 1—Liquid-phase oxygen concentration versus time (gas flow = 6.6 L/min; temperature = 17.5°C).

parameters. The gas-phase ozone concentration in the influent (Cgb) also was calculated and compared with the measured value. The iterative procedure was continued with new estimates of Cgt continued until the value of "$Cgb_{measured}$-$Cgb_{simulated}$" converged arbitrarily close to zero.

Results and Discussion

Oxygen Mass Transfer: Nonsteady-State Method. Figure 1 shows the oxygen concentrations as a function of time for a reaeration test, at the gas flow rate of 6.6 L/min. Experiments at other gas flow rates gave similar trends. Table 2 shows K_La values for tap water and reclaimed wastewater, along with the ratios of K_La values of reclaimed wastewater to tap water (alpha factor or α).

The mass-transfer rates vary with position in the column because of the plug-flow characteristics of both liquid and gas phases. As bubbles ascend the column, their diameter increases because of decreasing water pressure. Bubble coalescence further increases diameter, which decreases the specific interfacial area. Therefore, K_La may be larger at the bottom than at the top of the column. In full-scale reactors with lower height-to-diameter ratios, vertical mixing will be greater, deviating from plug flow and reducing this tendency. In Table 2, as expected, K_La increases with increasing gas flow rate because of the resulting greater specific surface area. It is often assumed that the relationship between K_La and superficial gas velocity (Ug) takes the form of a power law as follows (Bello et al., 1985):

$$K_La = aU_g^b \tag{10}$$

Where,

K_La = 1/min,
Ug = superficial gas velocity (m/h), and
a and b = constants to be determined.

The relationship was developed from a linear regression between the logarithms of K_La and Ug. The relationship was determined for tap water:

$$K_La = 0.076U_g^{0.569} (r^2 = 0.98) \tag{11}$$

And for reclaimed wastewater:

$$K_La = 0.040U_g^{0.8692} (r^2 = 0.98) \tag{12}$$

Where,

K_La = 1/min, and
Ug = superficial gas velocity = Qg/A = (m/h).

Alpha Factor. The main difference between reclaimed wastewater and tap water in this study is that the reclaimed wastewater contains more organic matter (Table 1). Organic matter and surface-active compounds can affect mass transfer in two ways: (1) by changing the mass-transfer coefficient (K_L); or (2) changing the interfacial area (a). Surface-active compounds tend to adsorb to the liquid/gas interface, which reduces the surface renewal of gas molecules and depresses the hydrodynamic activity. Accordingly, surface-active compounds typically reduce the K_L. When the surface-active compounds adsorb to the liquid/gas interface, they tend to lower the surface tension of water, which reduces the energy required to make smaller bubbles. The overall effect of surface-active compounds is to reduce bubble size, which increases a, while reducing K_L. Typically, the decline in K_L is not compensated by the increase in area, and there is a net reduction in K_La.

To quantify the effects of water quality on K_L, the alpha factor (α) was calculated as the ratio of K_La for reclaimed water ($K_La,_r$) to volumetric mass transfer coefficient for tap water ($K_La,_t$) or $\alpha = K_La,_r / K_La,_t$. Table 2 shows the values for the alpha factor that were obtained in this study.

A variety of conditions affect the alpha factor. Different aeration methods are affected differently with surfactants. Fine-pore diffusers (bubbles 3 mm or smaller) are more negatively affected than coarse-bubble diffusers and mechanical surface aerators (Stenstrom and Gilbert, 1981). The degree of treatment also affects alpha factors, because treatment tends to remove the surfactants

Table 2—Volumetric mass-transfer coefficient (K_La) values for oxygen transfer in tap water and reclaimed wastewater at different depths within the column at gas flow rates of 2.8, 4.7, 6.6, and 8.5 L/min ($K_La,_t = K_La$ for tap water; $K_La,_r = K_La$ for reclaimed wastewater).

	Tap Water $K_La,_t$ (min^{-1})				Reclaimed Water $K_La,_r$ (min^{-1})				
Gas Flow (L/min)	Top	Middle	Bottom	Average	Top	Middle	Bottom	Average	Average alpha
2.8	0.146	0.143	0.153	0.147	0.096	0.102	0.115	0.104	0.709
4.7	0.164	0.182	0.186	0.178	0.150	0.149	0.185	0.162	0.910
6.6	0.207	0.228	0.245	0.227	0.188	0.206	0.241	0.212	0.933
8.5	0.240	0.250	0.260	0.250	0.204	0.218	0.290	0.237	0.949

through oxidation or by adsorption to biosolids. Recently, Rosso and Stenstrom (2005) have shown that alpha factors are associated with sludge age or mean cell retention time (MCRT). Higher MCRT systems remove more surface active agents, and hence improve mass-transfer rates.

Table 2 also shows that the alpha factors are always less than 1.0, but increase with increasing gas flow rate. This phenomenon is caused by increasing turbulence as gas flow rate increases (Rosso et al., 2006). Organic compounds can affect the behavior of the bubbles and typically increase coalescence. Organic compounds that decrease coalescence may be more important at higher flow rates because more bubbles are present that might collide and cause more coalescence. Also surfactants, depending upon the characteristics, require a finite amount of time to adsorb to the bubble surfaces. At higher gas flow rates, the bubble surface renewal is greater, providing less opportunity for surfactants to build up. Hwang and Stenstrom (1985) have shown that alpha factors increased with increasing power input per unit volume. Eckenfelder and Ford (1968) and Gurol and Nekouinaini (1985) also noted similar effects.

Ozone Mass Transfer

Ozone Self-Decomposition in Tap Water. In organic matter-free tap water, the ozone self-decomposition reaction is the only possible reaction. When the pH is lower than 4, decomposition is negligible, but in tap water (approximately 6 to 7 pH) ozone self-decomposition can be significant (Gurol and Singer, 1982). The rate of self-decomposition is required to determine K_La. For clean water, it is assumed that ozone decomposition can be approximated as a first-order process (Zhou, 1995; Roustan et al., 1996):

$$\frac{dC}{dt} = -k_1 C \tag{13}$$

Where,

k_1 = first-order rate constant for ozone decomposition reaction (min^{-1}), and
C = ozone concentration in the liquid phase (mg/L).

The integrated form of Equation 13 is: $\ln(C) = \ln(C_0) - k_1 t$ with C_0 as the initial ozone concentration in the liquid phase.

The first-order assumption can be checked by plotting $\ln(C)$ versus time. If the relationship is linear, then the slope of the straight line is the decomposition rate constant. Four tests were conducted to determine the decomposition rate constant using least squares linear regression. A straight line was obtained for each of the decomposition experiments with a coefficient of determination greater than 0.95. Thus, a first-order decomposition reaction was observed for tap water in this study. Other researchers, such as Roth and Sullivan (1981), Hoigne and Bader (1983), and Zhou (1995), also found first-order decomposition in their experiments. Because the experiments were performed in a pilot plant treating water at ambient conditions, it was not possible to conduct all four experiments at the same temperature. To adjust the value of k_1 to 20°C, a relationship to temperature was used (Roth and Sullivan, 1983):

$$k_{1,(20^\circ C)} = 4 \times 10^{-9} k_{1,(T^\circ C)} \exp(5606/T) \tag{14}$$

Table 3 shows rate constants for ozone decomposition. The value of k_1 was 0.029 min^{-1} at pH 6 and 20°C, which is much lower than the values observed by Yurteri and Gurol (1987) for ozonation of natural waters. This difference indicates that a much slower ozone decay process occurred in the tap water used in this study. Yurteri and Gurol (1987) also developed an equation for the prediction of k_1:

$$k_1 = -3.98 + 0.66\ pH + 0.61\ log(TOC) - 0.42\ log(ALK/10) \tag{15}$$

Where,

TOC = total organic carbon (mg/L), and
ALK = alkalinity (mg/L as $CaCO_3$).

The k_1 value calculated using equation 15 is 0.013 min^{-1}, which is less than half of the observed value. The difference can be expected because Yurteri's test conditions were different from this study. They validated their equation for pH from 7 to 9, and alkalinity from 25 to 550 mg/L (as $CaCO_3$). Both the alkalinity and pH were lower in this study. The rate constant obtained here agreed more closely with Zhou's (1995) observed rate for deionized water, which was 0.028 min^{-1}.

Table 3—Summary of ozone decomposition rate constants at experiment conditions and 20°C (SD = standard deviation; T = time).

T, °C	16.2	19.4	18.6	19.5	Average ± SD
$k_{1,(T°C)}$, min^{-1}	0.0193	0.0313	0.0254	0.0309	
$k_{1,(20°C)}$, min^{-1}	0.0248	0.0326	0.0278	0.0319	0.0293 ± 0.00366

Nonsteady-State Method. In nonsteady-state reaeration testing, the liquid-phase concentration increases to an equilibrium concentration, which is a function of gas solubility and hydrostatic pressure. If a reaction is present, then the equilibrium concentration is reduced in proportion to the reaction rate (Roth et al., 1981; Sotelo et al., 1989). In a batch reactor, the ozone mass balance is given by a modified form of Equation 1:

$$\frac{dC}{dt} = K_La(C^* - C) - r_1 \tag{16}$$

Where,

r_1 = ozone decomposition rate ($r_1 = k_1 C^n$),
n, k_1 = empirically determined reaction coefficients,
C = liquid-phase ozone concentration, and
C^* = liquid-phase ozone concentration in equilibrium.

The liquid-phase ozone equilibrium concentrations increase with gas flow rate or K_La as shown in Figure 2. To use equation 16 to estimate the reaction coefficients, the liquid-phase ozone concentration was plotted for a range of concentrations and the reaction decomposition coefficients were found ($n = 1$, $k_1 = 0.029$ min^{-1} at pH 6 and 20°C in tap water). The ozone decomposition rate constant was then adjusted for different temperatures using Equation 14. The ozone mass-transfer coefficients were then obtained from equation 16 by rearranging:

$$dC/dt + r_1 = K_La(C^* - C)$$

And then plotting the left hand side ($dC/dt + r_1$) versus the ozone residual. The corresponding slope is the value of K_La. This procedure has been used before by Sotelo et al. (1989) and Roth and Sullivan (1981), and is also recognized by the American Society of Civil Engineers (ASCE) Standard Guidelines for Process Water

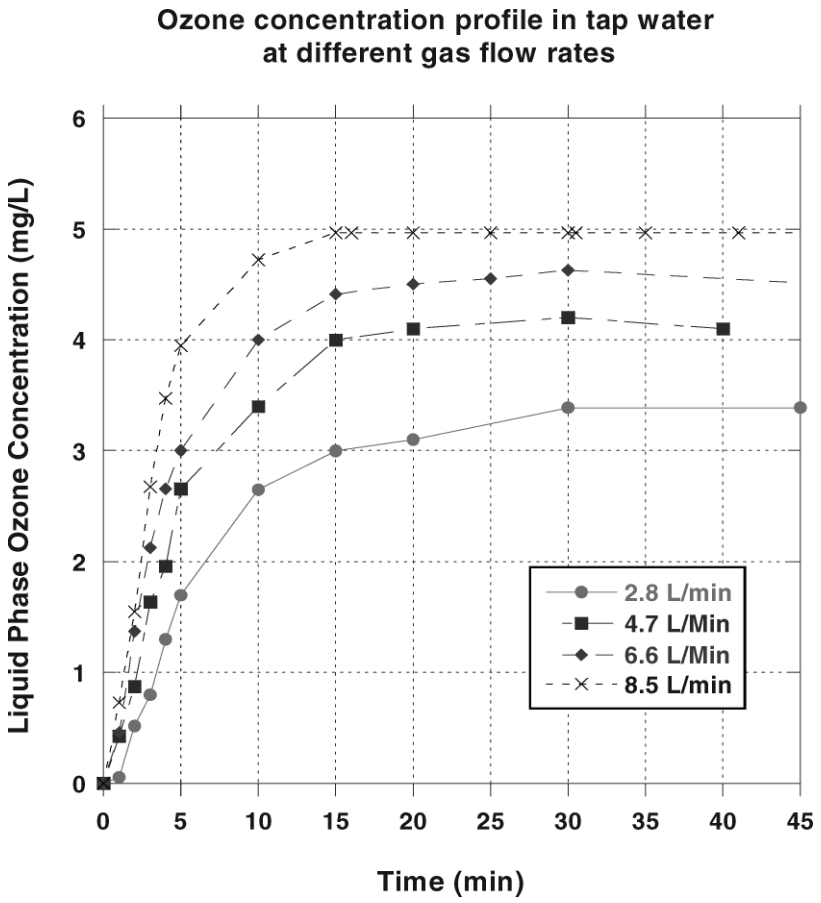

Figure 2—Gas flow rate influence on absorbed ozone concentration in tap water.

Testing (1997). Using this method, K_La was determined at four different gas flow rates. Table 4 shows the column average K_La adjusted to 20°C using parameter theta value of 1.024 (ASCE, 2006) together with the alpha values. The value of 1.024 is typically accepted for aeration and its use for ozone has been recommended by others (El-Din and Smith, 2003). The relationship between gas flow rate and ozone K_La was determined as before for oxygen:

$$K_La = 0.0636U_g^{0.586} (r^2 = 0.97) \quad (17)$$

For gas-liquid systems with rapid reactions in the liquid phase, such as ozonation reaction, it is possible that the mass-transfer coefficient is enhanced by the reaction in the liquid film surrounding the gas bubbles. The enhancement factor (E) is defined as the ratio of the ozone concentration gradient at the outer surface of the liquid film to that at the inner bound of the liquid film. A necessary condition to ensure that no reaction is occurring in the film for an irreversible first order reaction is:

$$Ha = (D_L w)^{0.5}/K_L < 0.3 \quad (18)$$

Where,

Ha = Hatta number,
D_L = diffusivity of the dissolved species, ozone (m^2s^{-1}),
w = reaction rate constant, either self decomposition for tap water or reaction with ozone demand for reclaimed water (s^{-1}), and
K_L = ozone mass-transfer coefficient (ms^{-1}).

The value of the K_L is estimated to be approximately 2.5×10^{-4} ms^{-1} (Laplanche et al., 1991). The diffusivity of the dissolved species is approximately 1.74×10^{-9} m^2s^{-1} at 20°C (Gurol, 1983). Thus, the maximum possible reaction rate constant to ensure no reaction in the liquid film is 194 min^{-1}, which is much larger than the reaction rate constant obtained in this study. This means enhanced mass transfer can be neglected. Several studies have shown similar results demonstrating that there is only minor enhancement of mass transfer even at high pH values where ozone decomposition is fast (Yurteri, 1988; Chang and Chian, 1981). In

Table 4—Volumetric mass-transfer coefficient (K_La) values at 20°C for ozone mass transfer at different points in the column at gas flow rates of 2.8, 4.7, 6.6, and 8.5 L/min ($K_La_{,t}$ = K_La for tap water; $K_La_{,r}$ = K_La for reclaimed wastewater).

Gas Flow (L/min)	Tap Water $K_La_{,t}$ (min^{-1})	Reclaimed Water $K_La_{,r}$ (min^{-1})	alpha
2.8	0.127	0.102	0.801
4.7	0.150	0.136	0.909
6.6	0.194	0.181	0.933
8.5	0.220	0.198	0.899

many chemical processes, it would be unusual for a gases being transferred to react only in the bulk liquid (Levenspiel, 1972). This situation is likely for most organic pollutants in water because the concentrations are low and noncatalytic reactions are typically slow at ambient temperatures (Chang and Chian, 1981).

Ratio of Volumetric Mass-Transfer Coefficients of Ozone to Oxygen (Psi). The ratios of experimentally determined volumetric mass-transfer coefficient for ozone to oxygen at various gas flow rates in both tap water and reclaimed wastewater are listed in Table 5 (Roberts et al., 1984). As expected, the ratio remains constant for all gas flow rates because the liquid film resistance dominates for both ozone and oxygen transfer. The average value of Psi (Ψ) was 0.86 for tap water and 0.88 for reclaimed water. According to the two-film theory, the ratio of mass-transfer coefficients is the ratio of diffusion coefficients for ozone and oxygen to the first power. The diffusion coefficients are 1.74×10^{-9} m^2s^{-1} and 2.09×10^{-9} m^2s^{-1} at 20°C, respectively, using the Wilke-Chang correlation. Thus, the theoretical ratio of K_Lao_3/K_Lao_2 is calculated to be around 0.83, which is only slightly different from what was found in this study (0.86 to 0.88). Penetration and surface renewal theories predict the mass-transfer coefficient to be proportion to the square root of the ratio of the diffusion coefficients, which equals 0.91. The experimental results fit well within the theoretical predictions based on gas transfer theories. Also, differences may arise from the method used to estimate diffusion coefficients because the Wilke-Chang correlation is only considered valid within ± 15%. This means that the possible range is 0.70 to 1.10. The ratio found in this study, 0.86 to 0.88, falls within the range.

Table 5—Volumetric mass transfer coefficient for oxygen (K_Lao_2) and for ozone (K_Lao_3) and the ratio of mass transfer coefficient for ozone to oxygen (Ψ) obtained by non-steady state method at various gas flow rates.

	Gas flow (L/min)	K_Lao_2 (min^{-1})	K_Lao_3 (min^{-1})	Ψ
Tap water	2.8	0.147	0.127	0.863
	4.7	0.178	0.150	0.845
	6.6	0.227	0.194	0.855
	8.5	0.250	0.220	0.880
Reclaimed wastewater	2.8	0.104	0.102	0.975
	4.7	0.162	0.136	0.844
	6.6	0.212	0.181	0.855
	8.5	0.237	0.198	0.834

In summary, the approximate relationships can be derived from the experimental results shown in Table 5, assuming two-film theory, as follows:

$$\psi = \frac{D_{O_3}}{D_{O_2}} = \frac{K_L a_{O_{3,r}}}{K_L a_{O_{2,r}}} = \frac{K_L a_{O_{3,t}}}{K_L a_{O_{2,t}}} \tag{19}$$

$$\alpha = \frac{K_L a_{O_{3,r}}}{K_L a_{O_{3,t}}} = \frac{K_L a_{O_{2,r}}}{K_L a_{O_{2,t}}} \tag{20}$$

Where,

$K_Lao_{3,r} = K_La$ for ozone in reclaimed wastewater,
$K_Lao_{2,r} = K_La$ for oxygen in reclaimed wastewater,

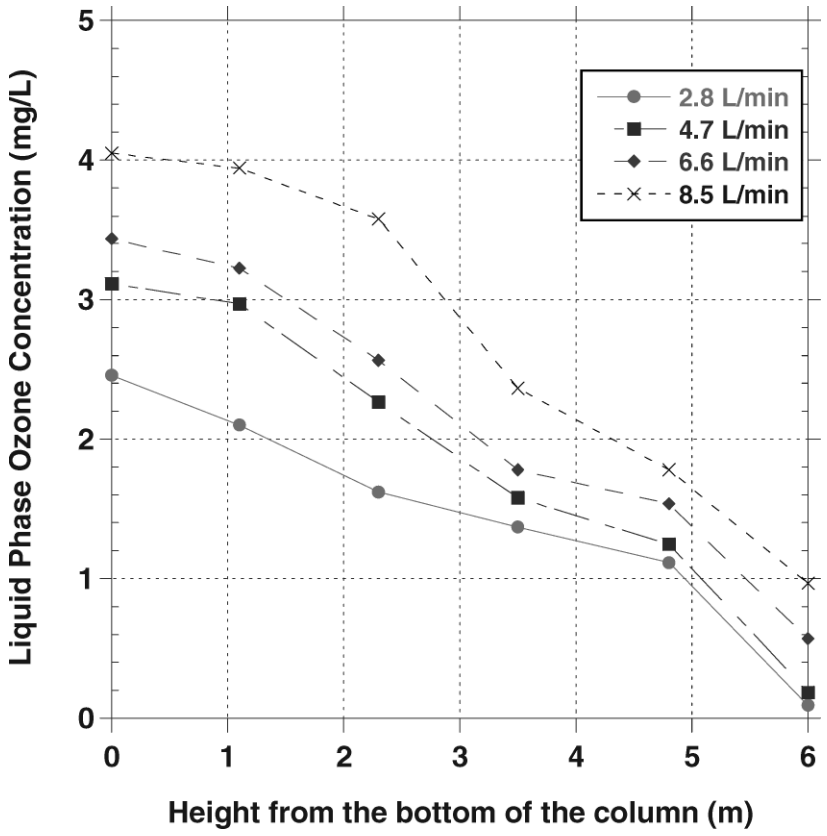

Figure 3—Measured liquid-phase ozone concentrations within the column in tap water.

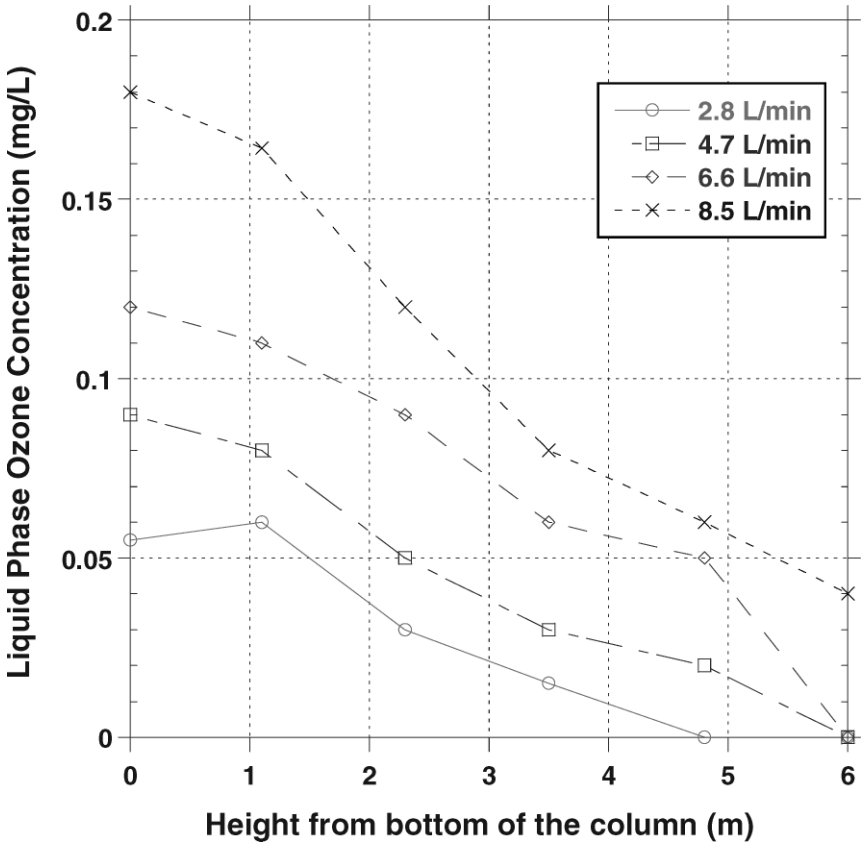

Figure 4—Measured liquid-phase ozone concentration along the column at different gas flow rates in reclaimed wastewater.

$K_L ao_{3,t} = K_L a$ for ozone in tap water, and
$K_L ao_{2,t} = K_L a$ for oxygen in tap water.

The most desired and most difficult to measure parameter, $K_L ao_{3,r}$, can be estimated by $K_L ao_{2,t}$ using a combination of Equations 19 and 20:

$$K_L a_{O_{3,r}} = \alpha \times \psi \times K_L a_{O_{2,t}} \tag{21}$$

The results suggest that ozone mass-transfer rate in reclaimed wastewater can be predicted by oxygen transfer rates in tap water. These rates can be obtained by a clean water test, which is much easier and more economical to perform.

Ozone Reaction Kinetics in Reclaimed Water. In this study, it has been shown that ozone self-decomposition can be successfully described as a first-order process in tap water. Pollutants in natural waters and reclaimed wastewater can react with ozone. There are two pathways to oxidize solutes: (1) direct reactions of organic or inorganic solutes with ozone molecules; and (2) indirect reactions of solutes with the ozone decomposition products (Staehelin and Hoigne, 1985). The rate of these reactions can differ by more than several orders of magnitude, depending on the structure of pollutants (Hoigne and Bader, 1983; Zhou, 1995). It is assumed that ozone consumption is dominated by direct reactions and that the rate of dissolved ozone consumption can be lumped into an overall expression that is first-order with respect to ozone concentration (Staehelin et al., 1985; Yuteri and Gurol, 1987; Watt et al., 1989; Roustan et al., 1996):

$$r = -wC \tag{22}$$

Where,

w = reaction rate constant.

Including the rate equation, the overall mass balance yields:

$$\frac{dC}{dt} = K_L a(C^* - C) - wC \tag{23}$$

At steady state, the accumulation term, dC/dt, goes to zero, leading to:

$$K_L a(C^* - C_{ss}) = wC_{ss}$$

Where,

C_{ss} = steady state liquid-phase ozone concentration.

By substituting into the overall mass balance equation:

$$\begin{aligned} dC/dt &= K_L a((wC_{ss}/K_L a) + C_{ss} - C) - wC \\ &= K_L a(C_{ss} - C) + w(C_{ss} - C) \end{aligned}$$

The new overall mass balance becomes:

$$\frac{dC}{dt} = (K_L a + w)(C_{ss} - C) \tag{24}$$

Assuming liquid-phase ozone concentration is zero at the start, equation 24 can be integrated as:

$$C = C_{ss}\{1 - \exp[(-K_L a - w)(t - t_0)]\} \tag{25}$$

Steady-state liquid-phase ozone concentration can be determined experimentally by sparging pure ozone-containing gas

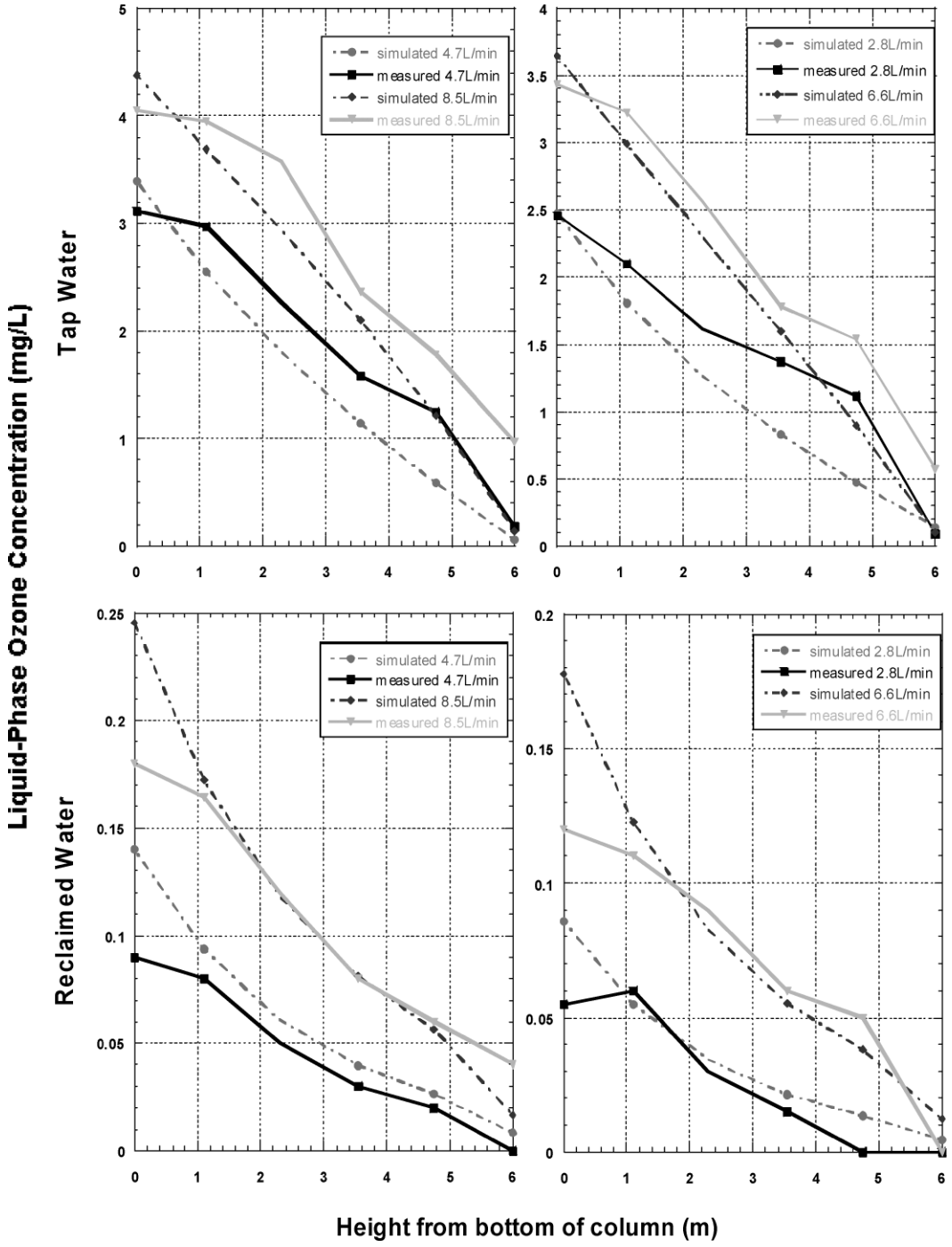

Figure 5—Comparison of measured and simulated ozone concentration profiles along the column at four gas flow rates (2.8 L/min, 4.7 L/min, 6.6 L/min, and 8.5 L/min) for both tap water (upper two) and reclaimed water (lower two).

through the liquid in the column until the liquid-phase ozone concentration reaches its plateau level. Volumetric mass transfer coefficient for ozone is predicted from the equation for oxygen mass transfer by assuming that ozone mass transfer is not enhanced by reactions involved in reclaimed wastewater. Then the ratio of mass transfer coefficient for ozone to oxygen of reclaimed water $(K_La_{O_3}/K_La_{O_2})_{\text{reclaimed water}}$ is equal to the ratio of tap water $(K_La_{O_3}/K_La_{O_2})_{\text{tap water}}$ from the former study of Ψ shown in Equation 19, 0.86 was adopted as the value of Ψ here. The value of K_La for oxygen in tap water was obtained earlier as $0.04\,U\text{g}^{0.8692}$, and therefore the coefficient for ozone can be given as:

$$K_La_{O_3} = 0.86 \times 0.04U_g^{0.8692} = 0.0344U_g^{0.8692} \qquad (26)$$

Thus, liquid-phase ozone concentrations as a function of time can be calculated by assigning a reaction rate constant (w) to minimize the sum of squares of errors (SSE) between observed and modeled ozone concentrations. The reaction rate constant that minimized the

Table 6—Comparison of measured and simulated ozone transfer efficiency and liquid-phase effluent ozone concentrations in tap water (Cg = gas-phase oxygen concentration; Cb = liquid-phase oxygen concentration at the bottom of reactor).

Gas flow rate (L/min)	8.5	6.6	4.7	2.8
Cg influent, mg/L	23.81	23.39	24.83	24.93
Cg effluent, mg/L				
Measured	6.72	6.22	4.82	4.5
Simulated	8.79	7.33	5.02	3.16
Simulation error, mg/L	2.07	1.11	0.20	1.34
Transfer efficiency (O_3TE), %				
Measured	71.8	74.4	80.6	81.9
Simulated	63.1	68.7	79.8	87.3
Simulation error, %	8.7	5.7	0.8	5.4
Cb effluent, mg/L				
Measured	4.05	3.44	3.12	2.46
Simulated	3.93	3.12	2.90	2.05
Simulation error, mg/L	0.12	0.32	0.22	0.41

Table 7—Comparison of measured and simulated ozone transfer efficiency and liquid-phase effluent ozone concentrations in reclaimed wastewater (Cg = gas-phase oxygen concentration; Cb = liquid-phase oxygen concentration at the bottom of reactor).

Gas flow rate, L/min	8.5	6.6	4.7	2.8
Cg influent, mg/L	7.25	7.18	7.68	7.45
Cg effluent, mg/L				
Measured	0.59	0.56	0.48	0.28
Simulated	1.03	0.96	0.85	0.64
Simulation error, mg/L	0.44	0.40	0.37	0.36
Transfer efficiency (O_3TE), %				
Measured	91.9	92.2	93.7	96.2
Simulated	85.8	86.6	88.9	91.4
Simulation error, %	6.1	5.6	4.8	4.8
Cb effluent, mg/L				
Measured	0.18	0.12	0.091	0.055
Simulated	0.25	0.19	0.15	0.090
Simulation error, mg/L	0.07	0.07	0.059	0.035

SSE was determined using an interval search between 0.5 and 5. The average reaction rate constant for four sets of experiments is 1.1 min^{-1}, which was found comparable with the results of other researchers with similar water quality. Roustan et al. (1996) obtained the pseudo first-order reaction rate constant to be 0.4–1.1 min^{-1} for water with TOC of 2 to 6 and pH of 7.8 to 8.1. Chang and Chian (1981) found the reaction rate constant to be 1.0 min^{-1} with a TOC value of 15 mg/L.

Ozone Concentration Simulation

Tap Water. Based on the previous experimental results for K_La for oxygen [$K_Lao_2 = 0.0636\ Ug^{0.586}\ min^{-1}$ ($r^2 = 0.97$)] and first-order rate constant for ozone decomposition reaction (0.029 min^{-1}), according to the method provided by Equations 8 and 9, ozone concentrations in both liquid phase and gas phase along the column were simulated using an iterative procedure. The K_La in the above equation is at 20°C and needed to be adjusted to tap water temperature. The value of liquid holdup h_L in Equations 4 and 5 was estimated by the relationship:

$$(1 - h_L) = 1.3 \times 10^{-3} U_g$$

Where,

U_g = superficial gas velocity (m/h) (Roustan et al., 1996).

Experimentally, the ozone residual monotonically decreases along column height. The highest ozone concentration was detected at the bottom of the column where ozone/oxygen gas entered and water left the reactor. Figure 3 shows the measured liquid-phase ozone concentrations along the column at different gas flow rates in tap water. Figure 5 (upper two) shows the comparison between measured and simulated liquid-phase ozone concentrations at various gas flow rates along the column. Comparisons of measured and simulated liquid-phase ozone concentrations in the effluent and ozone transfer efficiency are tabulated in Table 6. The trend of the simulated values matches that of the experimental data well. This suggests that the simulation approaches—including the plug-flow model, the ozone decomposition rate constant, and measured ozone volumetric mass-transfer coefficients—are reasonable. In general, the simulation values are pretty close to experimental results except for those at the bottom and top of the column, as seen in Figure 5 (upper two). The observed effects are probably caused by significant mixing at both ends of the column where gas and liquid enter and exit the column, whereas the simulations are based upon a plug-flow assumption. It is also observed that measured liquid-phase ozone concentrations are slightly higher than the simulated values. A possible explanation for the difference might be that micro-bubbles containing ozone were captured during sampling, despite the care taken.

Reclaimed Wastewater. Based on the previous experimental results for volumetric mass transfer coefficient for ozone ($K_Lao_3 = 0.0344\ Ug^{0.8692}$) as shown in Equation 26 and reaction rate constant (1.1 min^{-1}), according to the method given by Equations 8 and 9, ozone concentrations in both liquid phase and gas phase along the column were simulated using an iterative procedure. Other parameters are the same as in tap water part.

Figure 4 shows the measured liquid-phase ozone concentrations within the column at different gas flow rates in reclaimed wastewater. Figure 5 (lower two) shows the comparison between measured and simulated liquid-phase ozone concentrations at various gas flow rates along the column. The simulated and measured gas-phase ozone concentrations (*Cg*) are listed in Table 7. The simulated transfer efficiencies are close to measured values with a difference of less than 10%. The comparison of liquid-phase ozone concentrations in the effluent (*Cb*) between measured and simulated results are tabulated in Table 7. The absolute difference in *Cb* is small, ranging from 0.035 to 0.07mg/L.

Figure 6 indicates that applied ozone dose has to be greater than 1.2 gO_3/L water, to obtain a 0.1 mg/L liquid-phase ozone concentration in the effluent. The real value of applied ozone should be greater than 1.2gO_3/L water because the plug-flow model does not describe the concentration at the bottom of the column well where the liquid exits. This result compares well with the observation of Roustan et al. (1987), who found a dose of 1 mgO_3/L water is required to obtain a liquid-phase ozone

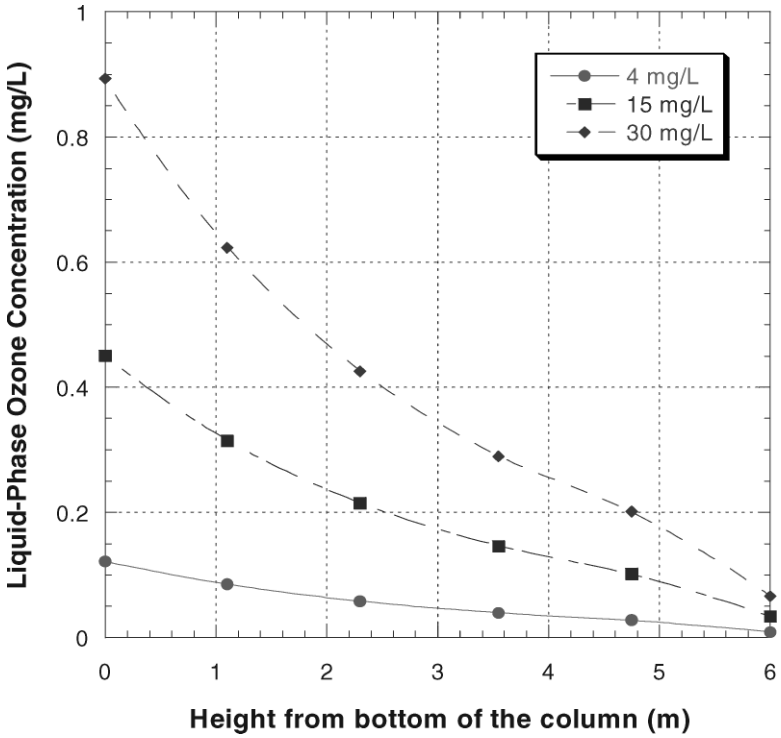

Figure 6—Effect of variation of influent gas-phase ozone concentration on simulated liquid-phase concentration profile (temperature = 16°C; gas flow = 8.5 L/min; reaction rate = 1.1 min^{-1}).

concentration of 0.1 mg/L. The difference in the required ozone dose between these two studies is caused by the differences in water quality and temperature. Tap water used by Roustan et al. (1987) was cleaner that the reclaimed water used here, with TOC value of 1.6 mg/L, and cooler, with a temperature of 5°C. Although the ozone reaction data was not provided by the author, there is no doubt that ozone decay is slower in their experiment.

Conclusions

Ozone and oxygen mass-transfer rates were measured in tap water and reclaimed wastewater at different gas flow rates using the nonsteady-state method. The mass-transfer rates were found roughly proportional to gas flow rates. Through the studies of psi and alpha (Ψ and α), the results suggest that ozone mass-transfer rates can be predicted by oxygen mass-transfer rates. The results also show that the contaminants in reclaimed wastewater do not appreciably reduce the mass-transfer rate.

A mathematical model was developed to describe transfer rates. The ozone decay reaction was included and accurately modeled as a pseudo first-order reaction between ozone and ozone demanding material. The model and experimental results agreed well.

Submitted for publication June 2, 2008; accepted for publication June 2, 2008.

The deadline to submit Discussions of this paper is April 15, 2009.

References

American Public Health Association (2005) *Standards for Examination of Water and Wastewater,* 21st ed.; American Public Heatlh Association: Washington, D.C.

American Society of Civil Engineers (2006) *Measurement of Oxygen Transfer in Clean Water*; American Society of Civil Engineers: New York.

American Society of Civil Engineers (1997) *Standard Guidelines for In-Process Oxygen Transfer Testing*; American Society of Civil Engineers: New York.

AWWA Research Foundation (1991) *Ozone in Water Treatment: Application and Engineering*; Lewis Publishers: Chelsea, Michigan.

Bader, H.; Hoigne, J. (1982) Determination of Ozone in Water by the Indigo Method: A Submitted Standard Method. *Ozone Sci. Eng.* **4** (4), 169.

Bello, R. A.; Robinson, C. W.; Moo-Young, M. (1985) Prediction of the Volumetric Mass Transfer Coefficient in Pneumatic Contactors. *Chem. Eng. Sci.* **40** (1), 53–58.

Brambilla, A. M.; Calvosa, L.; Monteverdi, A.; Polesello, S.; Rindohne, B. (1993) Ozone Oxidation of Polyethoxylated Alcohols. *Water Res.,* **27** (8), 1313–1322.

Chang, B. J.; Chian, E. S. K. (1981) A Model Study of Ozone-Sparged Vessels for the Removal of Organics from Water. *Water Res.,* **15** (7), 929–936.

Deckwer, W. D.; Burckhart, R.; Zoll, G. (1974) Mixing and Mass Transfer in Tall Bubble Columns. *Chem. Eng. Sci.,* **29** (11), 2177–2188.

Eckenfelder, W. W.; Ford, D. L. (1968) New Concepts in Oxygen Transfer and Aeration. In *Advances in Water Quality;* Gloyna E. F., Eckenfelder W. W., Jr., Eds.; University of Texas Press: Austin, Texas.

El-Din, M. G.; Smith, D. W. (2003) Mass Transfer Analysis in Ozone Bubble Columns. *J. Environ. Eng. Sci.,* **2** (1), 63–76.

Grasso, D. Ozonation Dynamics in Water Treatment: Autocatalytic Decomposition, Mass Transfer, and Effect on Particle Stability. Ph.D. Dissertation, University of Michigan, Ann Arbor, Michigan, 1987.

Gurol, M. D.; Nekouinaini, S. (1985) Effects of Organic Substances on Mass Transfer in Bubble Aeration, *Water Pollut. Control,* **57** (3), 235–240.

Gurol, M. D.; Singer, P. C. (1982) Kinetics of Ozone Decomposition: A Dynamic Approach. *Env. Sci. Technol.* **16** (7), 377–383.

Gruol, M. D.; Singer, P. C. (1983) Dynamics of the Ozonation of Phenol. 2. Mathematical Simulation. *Water Res.,* **17** (9), 1173–1181.

Hoigne, J.; Bader, H. (1983) Rate Constants of Reactions of Ozone with Organic and Inorganic Compounds in Water: Non-Dissociating Organic Compounds. *Water Res.,* **17** (2), 173–194.

Hsieh, C. C.; Ro, K. S.; Stenstrom, M. K. (1993a) Estimating Emissions of Twenty VOCs: Surface Aeration. *J. Environ. Eng.,* **119** (6), 1077–1098.

Hsieh, C. C.; Ro, K. S.; Stenstrom, M. K. (1993b) Estimating Emissions of Twenty VOCs: Diffused Aeration. *J. Environ. Eng.,* **119** (6), 1099–1118.

Hwang, H. J.; Stenstrom, M. K. (1985) Evaluation of Fine-Bubble Alpha Factors in Near-Full Scale Equipment. *J. Water Pollut. Control,* **57** (12), 1142–1151.

Ikehata, K.; El-Din, M. G. (2004) Degradation of Recalcitrant Surfactants in Wastewater by Ozonation and Advances Oxidation Processes: A Review. *Ozone: Sci. Eng.,* **26** (4), 327–343.

Khan, E.; Babcock, R. W.; Suffet, I. H.; Stenstrom, M. K. (1998) Method Development for Measuring Biodegradable Organic Carbon in Reclaimed and Treated Wastewaters. *Water Environ. Res.,* **70** (5), 1025–1032.

Khan, E.; Babcock, R. W.; Viriyavejakul, S.; Suffet, I. H.; Stenstrom, M. K. (1998) Biodegradable Dissolved Organic Carbon (BDOC) for Indicating Wastewater Reclamation Plant Performance and Treated Wastewater Quality. *Water Environ. Res.,* **70** (5), 1033–1040.

Laplanche, A.; LeSauze, N.; Martin, G.; Langlais, B. (1991) Simulation of Ozone Transfer in Water—Comparison with a Pilot Unit, *Ozone: Sci. Eng.,* **13** (5), 535–558.

LeSauze, N.; Laplanche A.; Martin, N.; Martin, G. (1993) Modeling of Ozone Transfer in a Bubble Column, *Water Res.,* **27** (6), 1071–1083.

Levenspiel, O. (1972) *Chemical Reaction Engineering*; John Wiley and Sons: New York.

Madireddi, K.; Babcock, R. W.; Levine, B.; Huo, T. L. Huo; Khan, E.; Ye, Q. F.; Neethling, J. B.; Suffet, I. H.; Stenstrom, M. K. (1997) Pilot-Scale Wastewater Reclamation at Lake Arrowhead California: An Overview. *Wat. Environ. Res.,* **69** (3), 350–362.

Marinas, B. J.; Liang, S.; Aieta, E. M. (1993) Modeling Hydrodynamics and Ozone Residual Distribution in a Pilot-Scale Ozone Bubble-Diffuser Contactor. *J. Am. Water Works Assoc.,* **85** (3), 90–99.

Mezzanotte, V.; Antonelli, M.; Citterio, S.; Nurizzo, C. (2007) Wastewater Disinfection Alternatives: Chlorine, Ozone, Peracetic Acid, and UV Light. *Water Environ. Res.,* **79** (12), 2373–2379.

Nakada, N.; Shinohara, H.; Murata, A.; Kiri, K.; Managaki, S.; Sato, N.; Takada, H. (2007) Removal of Selected Pharmaceuticals and Personal Care Products (PPCPs) and Endocrine Disrupting Chemicals (EDCs) during Sand Filtration and Ozonation at a Municipal Sewage Treatment Plant, *Water Res.,* **41** (19), 4373–4382.

Roberts, P. V.; Munz, C.; Dandliker, P. (1984) Modeling Volatile Organic Solute Removal by Surface and Bubble Aeration. *J. Water Pollut. Control,* **56** (2), 157–163.

Robson, C. M.; Rice, R. G. (1991) Wastewater Ozonation in the USA—History and Current Status—1989. *Ozone: Sci. Eng.,* **13** (1), 23–40.

Rosso, D.; Huo, D. L.; Stenstrom, M. K. (2006) Effects of Interfacial Surfactant Contamination on Bubble Gas Transfer. *Chem. Eng. Sci.,* **61** (16), 5500–5514.

Rosso, D.; Stenstrom, M. K. (2005) Comparative Economic Analysis of the Impacts of Mean Cell Retention Time and Denitrification on Aeration Systems. *Water Res.,* **39** (16), 3773–3780.

Rosso, D.; Stenstrom, M. K. (2006) Surfactant Effects on alpha-Factors in Aeration Systems. *Water Res.,* **40** (7), 1397–1404.

Roth, J. A.; Sullivan, D. E. (1981) Solubility of Ozone in Water. *Ind. Eng. Chem. Fund.* **20** (2), 137–140.

Roth, J. A.; Sullivan, D. E. (1983) Kinetics of Ozone Decomposition in Water. *Ozone: Sci. Eng.* **5** (1), 37–49.

Roustan, M.; Duguet, J. P.; Brette, B.; Brodard, E.; Mallevialle, J. (1987) Mass Balance Analysis of Ozone in Conventional Bubble Contactors. *Ozone: Sci. Eng.* **9** (3), 289–298.

Roustan, M.; Wang, R.Y.; Wolbert, D. (1996) Modeling Hydrodynamics and Mass Transfer Parameters in a Continuous Ozone Bubble Column. *Ozone: Sci. Eng.* **18** (2), 99–115.

Smith, D. W.; El-Din, M. G. (2002) Theoretical Analysis and Experimental Verification of Ozone Mass Transfer in Bubble Columns. *Environ. Technol.,* **23** (2), 135–147.

Sotelo, J. L.; Beltran, F. J.; Benitez, F. J.; Beltran-Heredia, J. (1989) Henry's Law Constant for the Ozone-Water System. *Water Res.,* **23** (10), 1239–1246.

Staehelin, J.; Hoigne, J. (1985) Decomposition of Ozone in Water in the Presence of Organic Solutes Acting as Promoters and Inhibitors of Radical Chain Reactions. *Environ. Sci. Technol.,* **19** (12), 1206–1213.

Stenstrom, M. K.; Gilbert, R. G. (1981) Effects of Alpha, Beta and Theta Factor upon the Design, Specification and Operation of Aeration Systems. *Water Res.,* **15** (6), 643–654.

Vilve, M.; Hirvonen A.; Sillanpaa, M. (2007) Ozone-Based Advanced Oxidation Processes in Nuclear Laundry Water Treatment. *Environ. Technol.,* **28** (9), 961–968.

Watt, R. D.; Kirsch, E. J.; Grady, C. P. L., Jr. (1989) Ozone Consumption Kinetics in Filtered Activated Sludge Effluents: A Modified Approach. *Water Res.,* **23** (4), 471–480.

Yurteri, C.; Gurol, M. D. (1987) Removal of Dissolved Organic Contaminants by Ozonation, *Environ. Prog.,* **6** (4), 240–245.

Yurteri, C. Removal of Organic Pollutants by Ozonation: Kinetics and Reactor Design. Ph.D. Dissertation, Drexel University, Philadelphia, Pennsylvania, 1988.

Zhou, H. Investigation of Ozone Disinfection Kinetics and Contactor Performance Modeling. Ph.D. Dissertation, University of Alberta, Edmonton, Alberta, Canada, 1995.